ACS APPLIED MATERIALS & INTERFACES

Research Article

www.acsami.org

Mechanical Properties of Plasma Immersion Ion Implanted PEEK for Bioactivation of Medical Devices

Edgar A. Wakelin,[*,†] Ali Fathi,[‡] Masturina Kracica,[§] Giselle C. Yeo,[∥,⊥] Steven G. Wise,[#] Anthony S. Weiss,[∥,⊥] Dougal G. McCulloch,[§] Fariba Dehghani,[‡] David R. Mckenzie,[†] and Marcela M. M. Bilek[†]

[†]Applied and Plasma Physics, School of Physics, The University of Sydney, Sydney, New South Wales 2006, Australia

[‡]School of Chemical and Biomolecular Engineering, The University of Sydney, Sydney, New South Wales 2006, Australia

[§]School of Applied Sciences, RMIT University, GPO BOX 476, Melbourne, Victoria 3001, Australia

[∥]School of Molecular Bioscience, The University of Sydney, Sydney, New South Wales 2006, Australia

[⊥]Charles Perkins Centre, The University of Sydney, Sydney, New South Wales 2006, Australia

[#]Applied Materials Group, Heart Research Institute, Newtown 2042 and Sydney Medical School, The University of Sydney, Sydney, New South Wales 2006, Australia

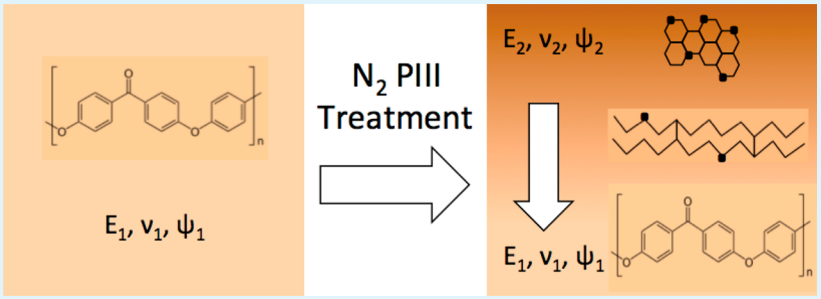

ABSTRACT: Plasma immersion ion implantation (PIII) is used to modify the surface properties of polyether ether ketone for biomedical applications. Modifications to the mechanical and chemical properties are characterized as a function of ion fluence (treatment time) to determine the suitability of the treated surfaces for biological applications. Young's modulus and elastic recovery were found to increase with respect to treatment time at the surface from 4.4 to 5.2 MPa and from 0.49 to 0.68, respectively. The mechanical properties varied continuously with depth, forming a graded layer where the mechanical properties returned to untreated values deep within the layer. The treated surface layer exhibited cracking under cyclical loads, associated with an increased modulus due to dehydrogenation and cross-linking; however, it did not show any sign of delamination, indicating that the modified layer is well integrated with the substrate, a critical factor for bioactive surface coatings. The oxygen concentration remained unchanged at the surface; however, in contrast to ion implanted polymers containing only carbon and hydrogen, the oxygen concentration within the treated layer was found to decrease. This effect is attributed to UV exposure and suggests that PIII treatments can modify the surface to far greater depths than previously reported. Protein immobilization on PIII treated surfaces was found to be independent of treatment time, indicating that the surface mechanical properties can be tuned for specific applications without affecting the protein coverage. Our findings on the mechanical properties demonstrate such treatments render PEEK well suited for use in orthopedic implantable devices.

KEYWORDS: *plasma immersion ion implantation, ion modification, PEEK, polyether ether ketone, nanoindentation, biocompatible, Elastic modulus*

INTRODUCTION

Plasma immersion ion implantation (PIII) is a promising surface modification technique for enhancing the properties of polymers.[1,2] Typical changes associated with PIII treatment include cross-linking,[3−5] increased Young's modulus[6,7] and oxidation,[8,9] and carbonization.[5,10,11] This technique has numerous practical advantages when compared to other ion implantation methods such as ion beam treatment (IB).[12] In PIII the workpiece to be modified is immersed into a plasma and a pulsed bias is applied directly to the workpiece (if conducting) or to a proximate electrode (if insulating). The pulse biased electrode accelerates ions from the plasma such that they are implanted into the workpiece, while in IB techniques ions are extracted from a plasma source via a series of meshes and accelerated as a beam to the workpiece. Although the ion energy spread is typically greater in PIII than

Received: July 15, 2015
Accepted: September 14, 2015
Published: September 14, 2015

DOI: 10.1021/acsami.5b06395
ACS Appl. Mater. Interfaces 2015, 7, 23029−23040

in IB techniques this is more than compensated by the ability to treat complex 3D shapes without rotation of the workpiece. A further significant advantage for insulating workpieces, such as PEEK orthopedic devices, is the fact that discharging between pulses occurs naturally through contact with electrons in the plasma without a requirement for an extra electron source. Furthermore, any plasma treatment system can be easily and relatively inexpensively upgraded to perform PIII by the addition of a pulsed power supply capable of providing pulsed bias in the kilovolt range. PIII is of particular interest for modifying high performance polymers such as polyether ether ketone (PEEK) for orthopedic uses. Enhanced polymer surface characteristics represent a significant advantage compared to metallic equivalents in the mechanical and biomedical industry with respect to reduced weight, production costs and the long-term viability of implantable devices.[13]

PEEK has been identified as a potential candidate for the next generation of orthopedic implants because of the similarity of its mechanical properties with those of bone and outstanding chemical properties.[14] Current orthopedic implants have limited lifetimes for a number of reasons.[15,16] One of the most prominent and preventable reasons for failure is bone resorption and aseptic loosening caused by a modulus mismatch between bone and metal implants, resulting in stress shielding.[17] The Young's modulus and Poisson's ratio of PEEK, however, are similar to cortical bone, reducing the risk of stress shielding, while possessing the strength to withstand bio-mechanical loads.

Unfortunately, PEEK is mildly hydrophobic and compared to titanium does not interact well with proteins and cells.[18,19] PIII treatment has been used here to bioactivate a surface layer of PEEK while leaving the bulk material unchanged. During PIII treatment, ions from a plasma are accelerated toward the sample surface by a pulsed negative bias. These ions impact the surface, dissipating energy and breaking bonds. The penetration depth of the ions is dependent on the pulsed bias, where a bias of −20 kV produces an implantation depth of ∼90 nm.[10] This treatment when applied to polymers creates a radical-rich hydrophilic surface with a long shelf life, capable of forming covalent bonds with bioactive proteins or peptides.[1] Surfaces decorated with robustly immobilized bioactive entities have great potential to actively stimulate favorable biological responses to implanted biomedical devices through signaling to local tissues. A recent application of this method induced osteogenesis by immobilizing a combination fibronectin/osteocalcin fusion protein on PIII treated polystyrene surfaces.[20]

An ideal surface treatment is one that produces a bioactive surface covalently bound to the substrate through a graded layer while not affecting the bulk properties of the substrate material. Previous studies have found that the PIII treatment of organic polymers results in surface hardening and cross-linking, where the degree of modification varies with depth within the treated layer,[5,10,21] and where details of compositional and structural changes depend on the specific polymer and plasma used. Increases in hardness and cross-linking combined with residual stresses introduced as a result of surface treatment tend to produce a more brittle surface.[22] This brittle nature is exhibited in the PIII treatment of soft polymers, for example polystyrene and polyethylene, where cracking is observed during aging due to a large modulus mismatch between the surface and the bulk.[10] This scenario is acceptable as long as the surface cracks do not approach the dimensions of a cell, and delamination of the modified surface layer does not occur. Previous studies of PIII treated PEEK with a hydrogen plasma have indeed found increased hardness and embrittlement.[23] In addition to avoiding a discontinuous depth profile change in the Young's modulus, the surface must also have a similar elastic recovery to prevent delamination under cyclical physiological strains. Fortunately, PIII treated polymers show an increase in elastic recovery after treatment indicating that delamination from cyclical loading is unlikely.[13,24] Despite the advantages of PIII treatment and promising mechanical characteristics of PEEK, modification of the modulus and elasticity of PIII treated PEEK have not yet been proven suitable for orthopedic applications.

Previous studies of the chemical changes of PEEK after PIII treatment using FTIR probed the top ∼1 μm of the surface.[25] This technique allowed for examination of oxidation and overall changes to the treated layer, but did not allow for isolation of the biointerface, or for depth profiling. Studies of other PIII treated polymers using X-ray photospectroscopy (XPS) were able to investigate the interface and provide a depth profile of chemical changes within the treated layer.[11,26] This technique can provide direct evidence to determine whether the PIII treated layer is graded and bonded to the underlying bulk polymer, or is discontinuous.

Previously reported chemical changes in PIII-treated polymers, such as polystyrene and polyethylene, have shown an increase in oxygen and nitrogen content, which is believed to be responsible for permanently increasing the surface energy and creating local environments that help stabilize the radicals within the modified layer.[1,27] PEEK however, contains a large amount of oxygen within its native structure and as such may not be affected in the same way. XPS of PIII treated PEEK is investigated here to understand the changes in surface chemistry resulting from the ion treatment both at the surface and throughout the treated layer.

This study investigates the surface mechanical and chemical changes as well as protein binding capability of PIII treated PEEK, with the aim of confirming that the surface is capable of immobilizing proteins and explaining how changes in mechanical properties of the polymer are related to the chemical modification after treatment.

MATERIALS AND METHODS

PEEK and PIII Treatment. Medical grade semicrystalline PEEK with a sheet thickness of 220 μm and density of 1301 kg m^{-3} was obtained from Victrex Manufacturing Ltd., Lancashire. PEEK sheets were cut into 5 × 2 cm strips for Instron measurements and cut into 1 × 1 cm strips for nanoindentation and XPS measurements. Samples were PIII treated for times between 240 and 1600 s, corresponding to ion fluences of 3 × 10^{15}− 2 × 10^{16} ions cm^{-2}. These treatment times were chosen to reflect treatments that have previously been shown to result in material characteristics that are highly dependent on ion fluence (240 s), not dependent on small changes of ion fluence (800 s), and independent of ion fluence (1600 s).[25,28] The nitrogen plasma consisting mainly of N_2^+, N^+ ions and neutral gas species was generated with an rf power of 100 W at a pressure of 2 × 10^{-3} Torr and directed toward the sample by use of magnetic field coils. Ions were accelerated with a pulsed bias voltage of −20 kV for pulse lengths of 20 μs applied at 50 Hz. During PIII treatment, the sample is immersed in the nitrogen plasma, and is therefore also exposed to UV radiation generated by the plasma, where the UV dose is dependent on the treatment time. To minimize surface charging and improve the homogeneity of the ion fluence, we used mesh-assisted PIII in this study. According to this method, a conducting wire mesh was placed a small distance above the sample and electrically connected to the

DOI: 10.1021/acsami.5b06395
ACS Appl. Mater. Interfaces 2015, 7, 23029−23040

sample stage. The mesh reduces both the variation in ion fluence at the surface,[10] and the electric field around the polymer sample, reducing the secondary electron emission, a major factor in surface charging during treatment.[29,30] During implantation, the ions are accelerated toward the mesh with a distribution of energies, where the maximum energy is equal to the pulsed bias voltage, in this case 20 keV.[29] Ions that pass through the holes in the mesh implant into the polymer sample. In this way, a high level of ion implantation is maintained, with a small amount of surface charging due to the implantation of ions, but without the surface charging that would arise from the emission of secondary electrons.

Previous studies have found that the surface chemistry continues to change significantly over the first week after treatment.[25] To reduce error, we aged all samples for 1 week before analysis.

Instron Tensile Testing. Macro-mechanical properties were investigated using an Instron 5543 testing machine in uniaxial tension with a 1 kN load cell. The length, width, and thickness of each sample were measured using digital callipers before each test. The Young's moduli were averaged over 6 specimens subjected to a single tension cycle. It was calculated as the slope of the stress strain curve between strains of 1.5 and 5%. The elastic energy recovery was calculated as the area enclosed by the unloading curve divided by the area enclosed by the loading curve and averaged over 6 specimen, where each sample underwent 200 loading−unloading cycles between strains of 1.5 and 3% at a physiologically relevant frequency of 0.25 Hz. All data were obtained using Bluehill3 software and analyzed using MATLAB.

Nanoindentation. Nano mechanical properties were determined using a Hysitron 950 Triboindenter fitted with a diamond Berkovich indentation tip. As this technique uses small loads and penetration depths, the deformation of the indenter must be accounted for when interpreting the load−displacement curve. In traditional mechanical testing, the Young's modulus is defined as the slope of the stress strain curve where the level of strain in the testing material is assumed to be far greater than that of the clamps holding the material in place. In nanoindentation the Young's modulus and Poisson's ratio play a role in the load−displacement curve, where the gradient is defined as the Reduced Elastic Modulus (E_r), and is given by

$$\frac{1}{E_r} = \frac{(1-\nu_i^2)}{E_i} + \frac{(1-\nu_s^2)}{E_s}$$

where E_i and ν_i are the Young's modulus and Poisson's ratio for the indenter, and E_s and ν_s are the corresponding values for the substrate. Because the Poisson's ratio of the PIII treated PEEK substrates is unknown, the modulus values determined from nanoindentation are E_r.

E_r was determined from the loading curves between depths of 5 and 25 nm and averaged over 25 indents. A depth profile was determined from a typical load−displacement curve and averaged over 5 nm bins from 5 to 90 nm.

Elastic energy recovery is also determined using nano indentation and is calculated in the same way as for Instron testing. Elastic strain recovery is observed here to follow the same trend as elastic energy recovery, and is a measure of the fraction of deformation recovered during the unloading cycle before the load decreases to zero. The stress load and unload rates used in this study were selected to be within the loading capacity of the apparatus and over a physiologically relevant range.

XPS and SEM. X-ray photoelectron spectroscopy (XPS) was performed using a K-Alpha Thermo Scientific system fitted with an Al Kα X-ray source. An argon flood gun was used during all measurements to minimize sample charging. In situ argon sputtering was utilized to obtain a depth profile with sputtering ion energies of 500 and 1000 eV.

To observe the effect of cyclical stresses on the treated surface layer, samples were sputter coated with 20 nm of gold and imaged with a Zeiss EVO 50 Scanning Electron Microscope, using an accelerating voltage of 5 kV.

Surface Coating with Tropoelastin (TE) and Detection with Enzyme-Linked Immunosorbent Assay (ELISA). PEEK samples were aged for 1 week after PIII treatment before being incubated overnight at 4 °C with 20 μg/mL TE. To identify protein that is covalently immobilized, we washed the samples in 5% w/v sodium dodecyl sulfate (SDS) in water solution at 80 °C for 10 min then rinsed in Milli-Q water. SDS is a detergent that is used to unfold proteins and to remove physically adsorbed proteins from surfaces. The SDS cleaning procedure is well-established in the literature[31−33] and more recently reviewed[1,34] as a test of covalent attachment to surfaces. SDS is an ionic surfactant that unfolds proteins and disrupts the forces responsible for physical adsorption, while leaving the covalent bonds intact.[35] Covalent bonding can be inferred when SDS washing under the same conditions completely removes protein from a more hydrophobic control surface with similar surface roughness as the test sample.[33,36] All samples were then incubated with 3% (w/v) bovine serum albumin (BSA). Surface-bound protein was detected with 1:2000 BA-4 mouse antielastin primary antibody (Sigma-Aldrich), followed by 1:5000 goat antimouse-HRP-conjugated secondary antibody (Sigma-Aldrich). Samples were then incubated in a 0.043 M ABTS substrate solution where the absorbance was measured at 405 nm after incubation at room temperature for 45 min.

RESULTS

Nanoindentation. Figure 1 shows E_r of untreated PEEK and PEEK PIII treated for 240, 800, and 1600 s. Indentation

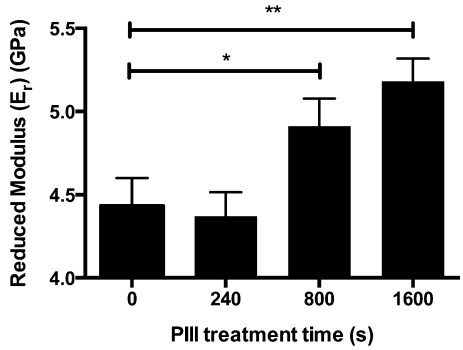

Figure 1. E_r of untreated PEEK and PIII treated PEEK subjected to treatments of 240, 800, and 1600 s (corresponding to ion fluences of 0.25×10^{16} to 2×10^{16} ions/cm^2). Measurements are averaged over 25 indents between depths of 5−25 nm and measured using a loading rate of 10 μN/s to a maximum load of 200 μN (* indicates significance of $p < 0.05$, ** indicates significance of $p < 0.01$).

was performed with a loading rate of 10 μN/s to a maximum of 200 μN, then immediately unloaded also at a rate of 10 μN/s. The measurements were averaged over 25 loading curves for each condition, and the displacement between 5 and 25 nm was fitted to ensure only the modulus of the modified layer was assessed. The E_r of the PIII treated surface shows no significant increase after 240 s of treatment. Longer treatment times, however, result in significant changes to E_r where the greatest change occurs after the longest treatment, increasing E_r from an untreated value of 4.43 to 5.18 MPa after 1600 s of treatment.

Figure 2 shows a typical depth profile of the E_r of untreated PEEK and PEEK PIII treated for 240, 800, and 1600 s. These samples were loaded in the same way as in Figure 1. Modulus values were calculated over 5 nm intervals for penetrations between 5 and 90 nm. The depth profile reflects the result depicted in Figure 1, where PEEK PIII treated for 800 and 1600 s display higher modulus values in the treated layer. The values measured from all samples converge at the ion penetration depth of approximately 80 to 90 nm indicating the depth of the PIII treatment. The modulus of all samples was increased with decreasing penetration depth between 5 and 20

DOI: 10.1021/acsami.5b06395
ACS Appl. Mater. Interfaces 2015, 7, 23029−23040

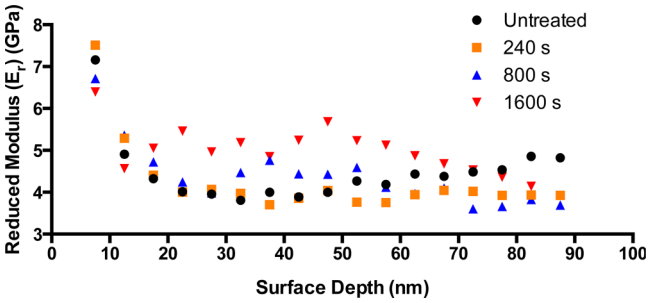

Figure 2. Typical depth profiles of E_r of untreated PEEK and PIII treated PEEK subjected to treatments of 240, 800, and 1600 s (corresponding to ion fluences of $0.25 \times 10^{16} - 2 \times 10^{16}$ ions/cm^2). Surface modulus was measured with a loading rate of 10 μN/s to a maximum load of 200 μN. PIII treatments of 800 and 1600 s produce a higher E_r throughout the treated layer. The E_r of all depth profiles shown here converge at the ion penetration depth of 80 to 90 nm.

nm. This feature is the result of an increased unloading strain rate associated with very low penetration depths and has been observed in other studies.[37]

Figure 3A shows typical load–displacement data for untreated PEEK and PEEK PIII treated for 240, 800, and 1600 s. The load was increased at a rate of 20 μN/s to a maximum load of 70 μN. The load was then held for 10 s before decreasing at a rate of 20 μN/s. The maximum load was chosen such that the loading–unloading cycle would occur within the PIII treated layer (top 80–90 nm). The area enclosed by the curve decreases with increased treatment time, indicating that the elastic energy recovery of PIII treated PEEK is greater than that of untreated PEEK when loaded at a rate of 20 μN/s. The elastic strain recovery also displays this trend after PIII treatment. Numerical values for the elastic recovery are presented in Figure 4.

Figure 3B shows typical load–displacement data for PEEK PIII treated for 800 s, where the load was increased at a rate of 20 μN/s to a maximum load of 70 μN, held for 10 s, then decreased at three different rates of 6.67, 20, and 100 μN/s. The area enclosed by the curve decreases with increasing strain rate indicating the elastic energy recovery of the material is strain rate dependent under these conditions. Elastic strain recovery is less pronounced under these conditions but follows the same trend.

Figure 4A shows the elastic recovery of untreated PEEK and PEEK PIII treated for 240, 800, and 1600 s. Samples were loaded at a rate of 20 μN/s to a maximum load of 70 μN, held for 10 s and then unloaded at three difference rates of 6.67, 20, and 100 μN/s. The elastic recovery is a measure of the fraction of energy recovered during unloading, and is defined as the area under the unloading curve divided by the area under the loading curve. The elastic recovery of PIII treated PEEK is increased compared to untreated PEEK in all cases ($p < 0.001$) from a minimum value of 0.48 for untreated PEEK to a maximum of 0.69 for PEEK PIII treated for 800 s.

Strain rate dependence of the elastic recovery can be observed in untreated PEEK between the highest and lowest unloading rates, however the effect is small ($\Delta = 0.01$). Changes in the elastic recovery are greater in PEEK PIII treated for 240 and 800 s where $\Delta = 0.03$ and 0.04 respectively. Samples treated for 1600 s, however, do not display strain rate dependent behavior.

Figure 4B shows data under the same conditions as Figure 4A, with the exception that the maximum load was increased to 200 μN. The effect is to probe deeper into the surface (~150 nm) and investigate the elastic recovery of the material beneath the PIII treated layer. Changes in the elastic recovery with respect to treatment time are still significant; however, they are far less in magnitude, indicating that the material beneath the treated layer is similar to untreated PEEK. Time-dependent changes to the elastic recovery are no longer observed under these conditions.

Macroscopic Mechanical Properties. The PEEK sheet used in this study has been drawn during production such that faint lines are visible in the direction of the long axis. Figure 5 shows the tensile Young's modulus of untreated and PIII treated PEEK tested perpendicular to the drawing direction. The Young's modulus increases with treatment time from 606 to 683 MPa. Some slipping may have occurred during the testing of untreated PEEK in the parallel direction compared to testing in the perpendicular direction as the clamps could grip the feint lines more effectively. However, after PIII treatment there was no significant difference between the perpendicular and parallel measurements. The relative increase in the tensile modulus of a sheet after PIII treatment is higher than expected when compared to the nanoindentation data. This increase may be the result of UV treatment from exposure to the nitrogen plasma, which results in deeper modification of the polymer compared to the ion bombardment.

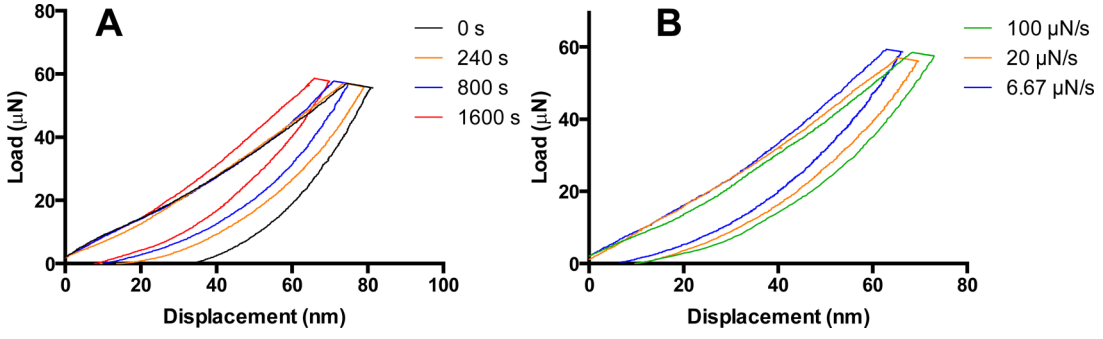

Figure 3. Typical load–displacement curves for: A) untreated PEEK and PIII treated PEEK subjected to treatments for 240, 800, and 1600 s (corresponding to ion fluences of $0.25 \times 10^{16} - 2 \times 10^{16}$ ions/cm^2). The load increased at 20 μN/s to a peak of 70 μN, was held for 10 s then decreased at 20 μN/s. B) PEEK PIII treated for 800 s loaded in the same way, but unloaded at 3 constant rates of 100 μN/s, 20 μN/s and 6.66 μN/s. Note in both A and B that the elastic strain recovery shows a similar trend to elastic energy recovery. A statistical analysis of the elastic recovery of the full data set is provided in Figure 4.

DOI: 10.1021/acsami.5b06395
ACS Appl. Mater. Interfaces 2015, 7, 23029–23040

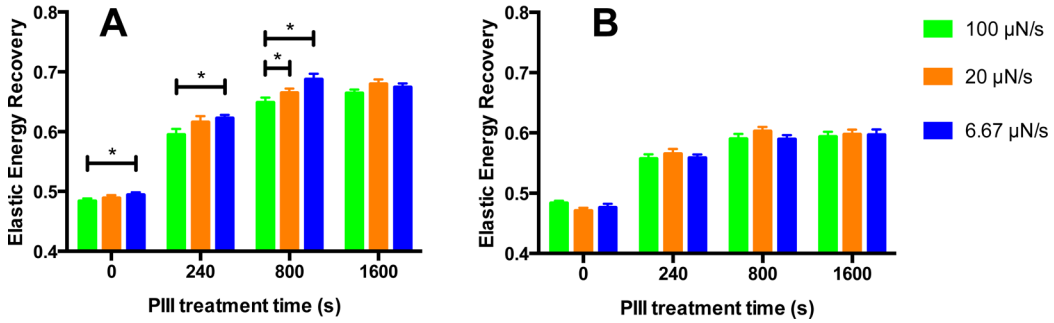

Figure 4. Elastic energy recovery of untreated PEEK and PIII treated PEEK subjected to treatments for 240, 800, and 1600 s (corresponding to ion fluences of 0.25×10^{16} to 2×10^{16} ions/cm^2). All samples were loaded at a rate of 20 μN/s to a maximum load of (A) 70 and (B) 200 μN, held for 10 s, then unloaded at three constant rates of 100, 20, and 6.66 μN/s. (* indicates significance of $p < 0.05$).

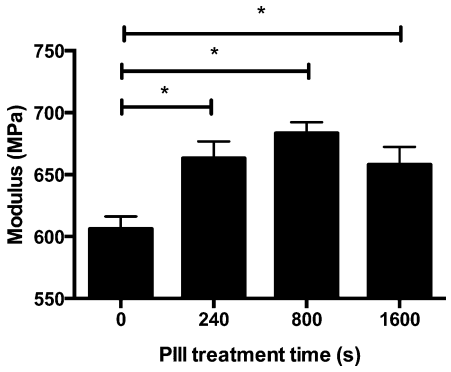

Figure 5. Tensile modulus of untreated and PIII treated PEEK. Samples were loaded at a strain rate of 0.5 mm/min to a max load of ~200 N. PEEK samples were tested perpendicular to the direction of drawing. (* indicates significance of $p < 0.05$).

Figure 6 shows the elastic recovery of untreated PEEK and PIII treated PEEK tested for 200 cycles and averaged over 6

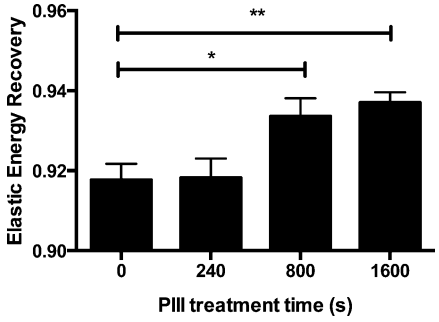

Figure 6. Elastic energy recovery of untreated and PIII treated PEEK over 200 tension cycles measured in an Instron 5543 at a rate of 0.25 Hz between strains of 2−5%. The elastic recovery of PIII treated PEEK increases with increased treatment time, and the effect is smaller than for nanoindentation. (* indicates significance of $p < 0.05$, ** indicates significance of $p < 0.01$).

samples between strains of 1 and 5% at a frequency of 0.25 Hz. The higher proportion of energy recovered here compared to the results from nanoindentation can be attributed to lower macroscopic sample testing strains. The elastic recovery again increases with treatment time; however, the change is less pronounced. This result is consistent with nanoindentation, as during Instron testing the entire thickness of the PEEK sheet was investigated as opposed to investigating the treated layer in isolation as in nanoindentation.

SEM of Treated Surface after 200 Cycles. The SEM images of samples after cyclical testing were used to determine the impact of the treated layer on delamination as a result of the mechanical testing. The results in Figure 7 show that, after 200 cycles, there is a negligible effect on untreated PEEK sample; however, cracking was observed on the PIII treated PEEK for 240 and 1600 s as a result of increased brittleness of the treated surface layer. On the other hand, these samples do not display any delamination, indicating that the ion activated surface layer is strongly bound to the substrate.

XPS. Figure 8 shows the carbon, oxygen and nitrogen XPS signals from untreated PEEK and PEEK PIII treated for 1600 s. All samples in the Figure have been etched for 10 s with a 500 eV argon beam to remove any adventitious carbon. The XPS peaks in this Figure have been fitted, and the details of the fits are compared to literature in Tables 1 and 2. The fitted peaks for untreated PEEK match the literature well, all expected peaks are present and exhibit a low concentration of contamination.

The C 1s signal of PIII treated PEEK, shown in Figure 8 B shows a large central carbon−carbon peak with a normalized bond energy of 285 eV, and an asymmetric elongated tail toward higher energies. Assigning peaks to this signal is difficult because a large range of organic functional groups could be present in the surface. The relative concentrations and chemical groups at the surface of the PIII treated layer are not known in detail; however, it is clear from the continuous tail in the signal that many of the groups have chemical shifts that cannot be distinguished from one another. To provide an estimate of the groups that may be present, we used 6 fits such that the residual signal was close to zero. These fits may be composed of a number of groups and have been labeled as such. Using these likely fits, corresponding groups were also fitted to the O 1s and N 1s signals.

The depth profile of the atomic percentage of nitrogen as a function of etching time in the treated surface is shown in Figure 9A. Increased treatment time produces an increased nitrogen atom % in the treated layer. Ion penetration, however, is primarily a property determined by the pulsed bias during treatment; correspondingly, the penetration depth of nitrogen does not increase with increased treatment time. Nitrogen concentration decreases with etch time (depth) where the concentration approaches zero after approximately 300 s of etching.

The relative concentrations of the functional groups within the nitrogen N 1s signal are shown in Figure 9B as a function of treatment time after 10 s of etching. Untreated PEEK does not contain nitrogen levels above noise, as such all nitrogen groups

DOI: 10.1021/acsami.5b06395
ACS Appl. Mater. Interfaces 2015, 7, 23029−23040

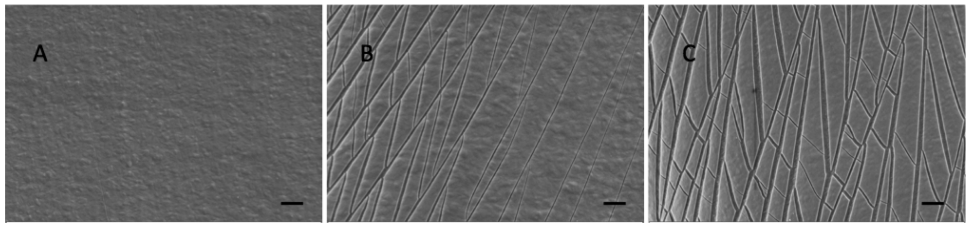

Figure 7. SEM images of (A) untreated PEEK, (B) PEEK PIII treated for 240 s, and (C) PEEK PIII treated for 1600 s showing cracking of the treated surface after 200 loading cycles. Note that the treated layer does not exhibit any peeling from the substrate. Scale bar = 2 μm.

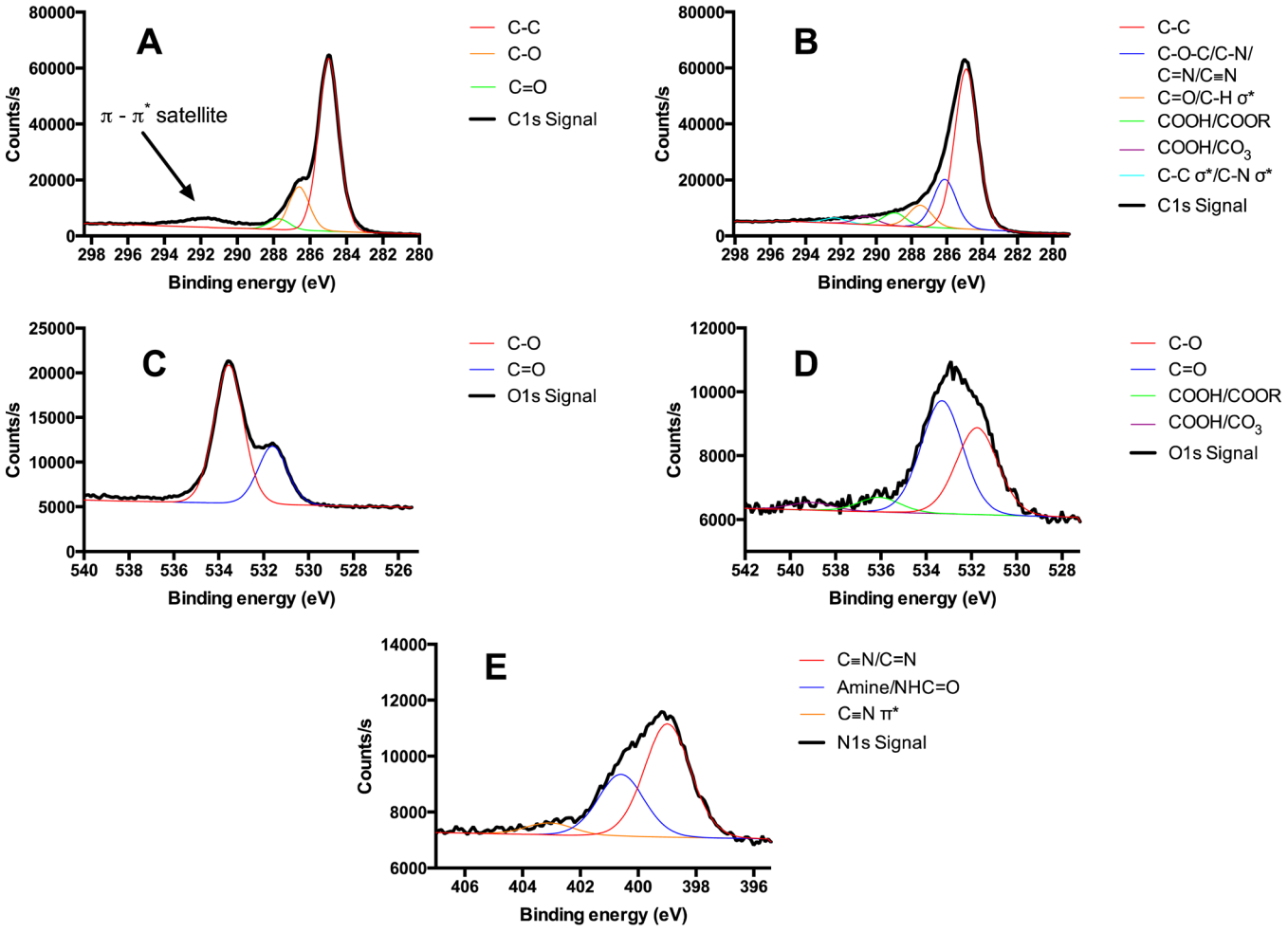

Figure 8. Fitted XPS signals of untreated PEEK (A) C 1s and (C) O 1s signals; 1600 s PIII treated PEEK (b) C 1s, (D) O 1s, (E) and N 1s signal, respectively. All samples were etched for 10 s with a 500 eV beam to remove any adventitious carbon.

Table 1. Fitted XPS C 1s and O 1s Peaks of Untreated PEEK Compared to Values from Literature

UT PEEK (10 s etch 500 eV)	peak assignment	binding energy (eV) (±0.1 eV)	literature values[38,39]	rel area
oxygen	O═C	531.6	531.6−532.5	0.30
	O−C	533.6	533.8−534.8	0.70
carbon	C−C	285	284.9−285.0	0.76
	C−O−C	286.6	286.3−286.8	0.19
	C═O	287.7	287.1−287.7	0.05
	shake up	291.6	291.6−292.0	

are given relative fractions of zero. Short treatment times predominantly produce nitrile and imine groups, further treatments produce higher proportions of amine groups that then saturate after 800 s of treatment. A small fraction of charged amine groups are produced, but the concentration is not dependent on treatment time.

Figure 10A shows the depth profile of the atom % of oxygen as a function of etching time and is compared to the theoretical atomic percentage of the PEEK monomer. Untreated PEEK shows an increased oxygen concentration compared to that expected from the monomer, which is probably a result of oxidation occurring during manufacture rather than contamination as the overall C 1s and O 1s XPS signal matches that of PEEK, nor is this a feature of polymer orientation, as the etching times investigated cover a depth range far greater than the width of the polymer chain. Oxygen concentration with zero etching on PIII treated samples is represented by 1 s of etching to allow the data to be plotted on a logarithmic scale.

DOI: 10.1021/acsami.5b06395
ACS Appl. Mater. Interfaces 2015, 7, 23029−23040

Table 2. Fitted C 1s, O 1s, and N 1s Peaks for PEEK PIII Treated for 1600 s Compared to Values from Literature

PIII 1600 PEEK (10 s etch 500 eV)	peak assignment	binding energy (eV) (±0.1 eV)	literature values[38−41]	rel area
oxygen	O−C	531.7	533.8−534.8	0.39
	O═C	533.3	531.6−532.5	0.51
	N_2O/COOH	536.1	536.0−536.3	0.07
	CO_3/COOH	539.1	539.0−539.2	0.03
carbon	C−C	284.9	284.9−285.0	0.62
	C−O−C/C−N/C═N/C≡N	286.1	286.3−286.8	0.19
	C═O/C−H σ^*	287.5	287.1−287.7	0.09
	COOH/COOR	289.0	289.3−290.5	0.05
	CO_3/COOH	290.6	290.0−291.0	0.03
	C−C/C-N σ^*	292.3	291.6−292.0	0.02
nitrogen	nitrile/C═N	399.0	397.8−399.0	0.61
	amine/NHC═O	400.6	400.6−401.9	0.33
	nitrile π^*/ charged amine	403.1	402.0−406.0	0.06

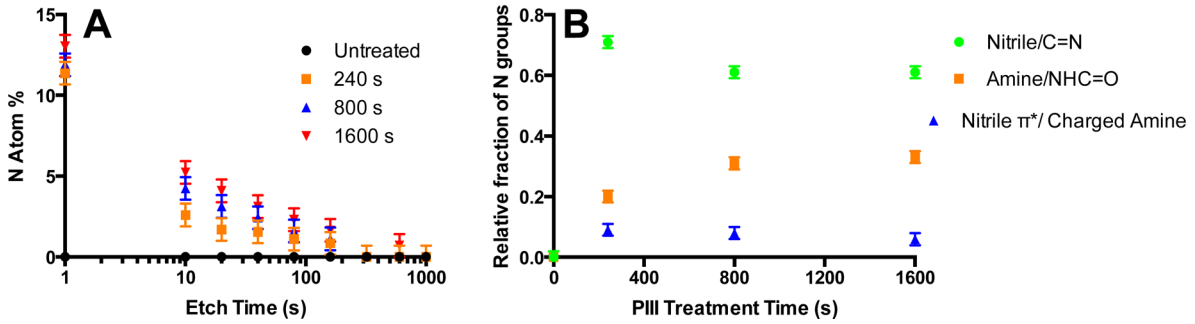

Figure 9. Breakdown of the nitrogen N 1s signal showing (A) depth profile of nitrogen as a function of etch time (etch energy of 1000 eV) in untreated PEEK and PEEK treated for 240, 800, and 1600 s. Increased treatment time increases the nitrogen concentration in the surface, however increased treatment times do not lead to increased nitrogen penetration depth. (B) Relative concentration of nitrogen bonding environments as a function of PIII treatment time after 1000 eV etching for 10 s. The dominant components are nitrile and amine groups that increase with treatment time and saturate after 800 s of treatment.

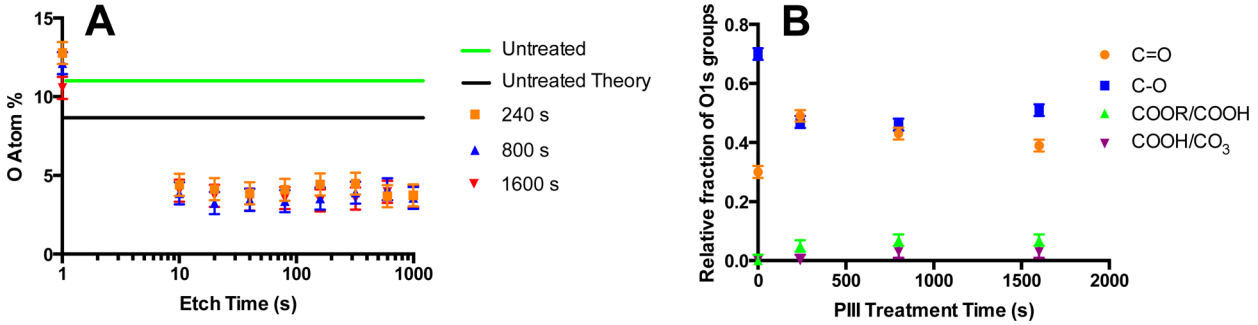

Figure 10. Breakdown of the oxygen O 1s signal showing (A) depth profile of oxygen as a function of etch time (etch energy of 1000 eV) in untreated PEEK and PEEK PIII treated for 240, 800, and 1600 s. Zero etch time is represented here as 1 s of etching for ease of representation on a logarithmic scale. PIII treatment reduces the total oxygen content and is not treatment time or etch time dependent. (B) Relative concentration of oxygen bonding environments in O 1s signal as a function of PIII treatment time after 1000 eV etch for 10 s. The dominating components, C═O and C−O groups, change relative to each other as a function of PIII treatment time.

The oxygen concentration with zero etching is unchanged compared to untreated PEEK and indicates that radicals emerging from the treated layer react with atmospheric oxygen to replace the oxygen that has been displaced during treatment. The net result after treatment is that the carbon atom % at the surface decreases. The oxygen concentration decreases dramatically below the surface (etch time ≥10 s) to ∼4.5% with PIII treatment. This value remains relatively constant throughout the PIII treated layer and does not return to the untreated value at or beyond the penetration limit of the nitrogen ions.

Relative concentrations of the functional groups within the oxygen O 1s signal are shown in Figure 10B as a function of treatment time after 10 s of etching. Before treatment, the oxygen in the surface is in the form of either C−O or C═O in relative fractions of 70:30, similar to the atomic percentage of oxygen in the monomer. With short PIII treatment times the concentration of C−O decreases to approximately 45% of the oxygen content before increasing to 50% after 1600 s of treatment. The C═O concentration increases with short treatment times to 50%, before decreasing to 40% after 1600 s of treatment. Other groups such as carboxylic groups and carbon trioxide are not present in the untreated polymer but do

DOI: 10.1021/acsami.5b06395
ACS Appl. Mater. Interfaces 2015, 7, 23029−23040

appear after treatment where the concentration increases with treatment time. However, the concentrations of these groups remain low.

Protein Immobilization. TE is used as a model protein as it is a promising candidate to enhance the biocompatibility of implantable devices because it interacts with a range of cell surface receptors.[42,43] Attachment of TE to untreated and PIII treated PEEK surfaces is shown in Figure 11. Samples not

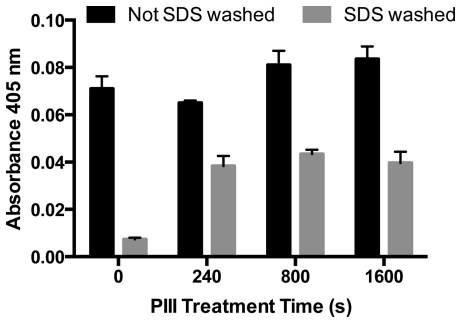

Figure 11. ELISA signal of TE bound to untreated and PIII treated PEEK surfaces. After SDS washing, TE is almost entirely removed from untreated PEEK but not from PIII treated PEEK indicating a high level of covalent protein immobilization on the treated surface.

washed in SDS show similar levels of protein adsorption. Following SDS washing, the TE signal of untreated PEEK is reduced to background, indicating that the protein was physisorbed but not covalently bound to the surface. SDS washing of protein coated PIII treated PEEK however, retained 50−60% of TE indicating a high level of covalent attachment. The ELISA signal after SDS washing does not increase with increased treatment time in the range investigated here, indicating that all treatments produce equivalent surfaces with respect to protein immobilization.

DISCUSSION

Modulus. The E_r of untreated PEEK was measured as 4.4 GPa, and is comparable to values reported in literature.[44] Increased modulus as a result of PIII treatment was treatment time dependent, such that longer treatment times result in a greater increase. This trend was also observed in the depth profile, where long treatment times show higher values within the treated layer. The E_r values, however, converge to those of the untreated sample at greater depths (~90 nm), indicating that the thickness of the treated layer is not treatment time dependent, and that the mechanical modification is contained within a surface layer, where the underlying PEEK remains untreated.

The depth profile of nitrogen penetration supports the finding that treatment depth is not dependent on treatment time, but indicates that nitrogen concentration, corresponding to the intensity of modification, does increase with treatment time. Decreasing nitrogen concentration with etch time (depth) indicates that the level of material modification decreases with depth. Reduced levels of modification with increasing depth produces a graded layer of PIII modified polymer and unmodified PEEK. This feature is beneficial as it allows for strong integration between the treated layer and untreated substrate. Well-integrated surface structures such as these prevent delamination that result in exposure of untreated material that can lead to adverse tissue responses and early implant failure.

Macroscopic testing of untreated PEEK produced a tensile elastic modulus in the range of 580 to 620 MPa. The relative increase in tensile modulus of PIII treated PEEK is less than that observed during nanoindentation. This result can be explained by the ratio of the volume of the PIII treated layer of PEEK to that of the untreated PEEK bulk in the test samples. The PIII treated surface represents 0.05% of the total cross-sectional area, and the effect on the modulus is correspondingly lower. Scaling this effect to a physiologically relevant geometry, the change in tensile modulus of the treated layer will have a negligible effect on the tensile modulus; thus PIII treated PEEK structures retain mechanical characteristics that will prevent stress shielding in orthopedic implants.

The increase in modulus post-PIII treatment has previously been attributed to increased cross-linking in PEEK[23] as well as in other polymers.[3,22] XPS oxygen and carbon data of untreated PEEK presented in Figure 8 is consistent with previously reported values in literature.[38,39] The C 1s signal of the PIII treated surface, however, is significantly different from that of untreated PEEK. A high binding energy tail has been introduced, indicating that a large, almost continuous, variety of chemical environments are present such that the individual signal shifts cannot be resolved. The larger variety of carbon and oxygen chemical environments after treatment indicates an increased level of cross-linking that hinders polymer chain slip, resulting in a surface with higher stiffness.

Radical production as a function of PIII treatment time has previously been shown to saturate after 800 s of treatment under the treatment conditions used here.[25] Increased radical concentration will increase the amount of cross-linking and affect the type of nitrogen species that can form. Therefore, the relative concentration of nitrogen species shown in Figure 9B is related to the level of cross-linking within the PIII structure. At low concentration the probability of radicals on different polymer chains reacting together through nitrogen atoms is low. This results in reactions with nitrogen contained within a single chain such that the dominating nitrogen compounds are nitrile groups. When the radical concentration increases, however, the likelihood of radicals on different chains reacting through nitrogen atoms rises, allowing amine groups to form. There will always be a small proportion of more exotic nitrogen containing groups as a result of PIII treatments due to the high-energy random nature of the atomic collisional processes that occur during PIII treatment. The total concentration of nitrogen has been shown to decrease with time after treatment,[25] indicating that these groups are not stable and ultimately form volatile compounds and are released from the surface.

Covalent protein immobilization is achieved here through reactions with carbon-centered radicals on the surface. Previous studies investigating nanoscale modification of PIII treated PEEK and other polymers have shown insignificant changes to the surface topography, indicating that the additional protein immobilization, is purely due to reactions with radicals.[25,45] This immobilization prevents protein exchange, via the Vroman effect during BSA incubation,[46] and combined with an increased polar surface energy,[25,26] improves protein stability on the surface. Immobilization of TE on the PIII treated PEEK surfaces was found to be independent of treatment time in the range investigated, indicating that all treated surfaces here are suitable for protein interaction. In contrast, the Young's

DOI: 10.1021/acsami.5b06395
ACS Appl. Mater. Interfaces 2015, 7, 23029−23040

modulus of the PIII treated surface increased with treatment time. This effect means that PEEK surfaces can be bioactivated with relatively short PIII treatment times, and that the mechanical properties of the surface can be tuned for specific applications based on the treatment time.

Elastic Recovery. The fraction of energy recovered after an indentation test (termed here the elastic energy recovery) is defined as the area under the unloading curve divided by the area under loading curve. The values shown for untreated PEEK in Figure 4A vary in the range of 0.48−0.49 and is comparable to values previously reported in literature.[13] PIII treatment increases the elastic energy recovery of the treated surface in all cases and is dependent on treatment time; however, this effect saturates after 800 s of treatment. Increases in elastic energy recovery such as these, after PIII treatment have been observed in PEEK[13] and other polymers[6] exposed to various plasma treatments. The increase in elastic energy recovery can be attributed to carbonization and cross-linking within the surface layer. Cross-linking reduces plastic flow of the material by reducing slip between polymer chains. During deformation, the energy is stored in strained covalent bonds that are able to recover after the indentation stress is removed, increasing the elastic energy recovery.

Instron cyclical testing of PEEK (Figure 6) also shows an increase in the elastic recovery with PIII treatment. This effect, similar to the case of tensile modulus, is reduced when compared as a fraction of the original value to changes in the elastic recovery during nanoindentation. This effect can also be attributed to the small volume occupied by the treated layer compared to the sheet as a whole. A small increase in elastic recovery is beneficial and not expected to result in delamination of the treated surface. Strains above normal physiological strains, of approximately 0.3−0.4%,[47] were chosen to test the durability of the PIII surface. Images of these samples after straining (Figure 7) display cracking, indicating an increased brittleness resulting from PIII treatment; however, there is no indication of peeling or delamination of the treated surface from the substrate. Increased elastic recovery and the presence of cracking indicates a robust surface where exposure of untreated PEEK, with the potential to result in adverse biological reactions, through cyclical loading is highly unlikely.

The increase in elastic energy recovery observed with decreased unloading rate shown in Figure 4A for untreated PEEK and PIII treatment times of 240 and 800 s indicates that there is a time dependent aspect to the deformation. The strain rate dependence of untreated PEEK is significant, although the effect is very small (increase in recovery of 1%). The time dependence can be attributed to deformation being comprised of two components: (1) elastic deformation, where energy is stored in covalent bonds and crystalline regions, and (2) plastic deformation associated with polymer flow. Elastic deformation dominates the elastic recovery; however, some recovery from polymer flow may occur as a result of residual stresses in the structure.

The effect of time dependence on elastic recovery increases for 240 and 800 s of PIII treatment. In these cases, cross-linking is introduced (but not to saturation) such that polymer flow cannot occur as readily as in the untreated polymer. This scenario will increase the proportion of elastic deformation and increase the residual stresses in the plastically deformed and cross-linked regions. When the indenter is withdrawn from the sample, the elastically deformed regions will recover immediately; however, the regions of plastic deformation under tensile stress from the cross-linked structure will recover over a longer time period. Surfaces treated for 1600 s result in further increased cross-linking such that the treated layer is effectively fixed in position preventing polymer flow. In this case, low levels of strain will be highly elastic, such that any plastic deformation will be irreversible and not time dependent.

Previous studies have found that PIII treatment of organic polymers (including PEEK) produces a hydrogenated amorphous carbon (a-C:H) surface layer.[48−50] Elastic recovery of a-C:H is known to be time dependent where lower levels of hydrogenation, and introduction of nitrogen, exhibit more time dependence such that pure amorphous carbon (a-C) displays a highly time dependent elastic recovery.[51] It would be expected that longer PIII treatment times, resulting in a more highly treated layer, would result in a greater time dependence of the elastic recovery. This characteristic is not seen here, and that may be attributed to the continuing presence of oxygen and hydrogen in the treated surface layer, such that it is not well approximated by a-C, or a-C:N; combined with effects due to the untreated PEEK substrate below the treated surface layer. Measurements of the elastic recovery of a-C:H are usually performed on silicon wafers with a relatively high modulus that contributes very little to the deformation. In this study, however, the substrate is bound through a graded layer to untreated PEEK, therefore effects from the stress field penetrating into the less treated and untreated regions will further reduce the time dependence of these results.

Figure 4B confirms that the surface layer under investigation in Figure 4A is mostly attributed to the PIII treated surface. During indentation in Figure 4B, the tip penetrates the treated layer and then continues through to the untreated substrate. The results show that the elastic recovery of the PIII treated samples decrease to a level closer to that of untreated PEEK and that the time-dependent recovery also becomes insignificant. Changes to the elastic recovery such as these provide further evidence that the PIII surface treatment does not penetrate deep into the substrate, and that the bulk mechanical properties required for orthopedic implantation are preserved in PEEK.

Oxygen Concentration. The oxygen concentration of PEEK (shown in Figure 10A) decreases significantly after PIII treatment and is not dependent on treatment or the subsequent etching time during analysis (at least to the depths studies here). This indicates that the same decrease in oxygen concentration is seen throughout the treated layer and at depths much greater than the ion penetration. The process resulting in the removal of oxygen is not, therefore, mediated by the ion bombardment or radical reactions that affect only the treated layer, and due to the depth of modification, it also cannot be attributed to the reorientation of polymer chains after treatment as has been observed in argon plasma treatment of PET.[52] Irradiation by ultraviolet (UV) photons generated in the plasma may account for modification of the PEEK at deeper levels than the ion bombardment.[53] This scenario is markedly different from other ion implantation techniques such as IB treatment[54] because the sample is immersed in the plasma during treatment and therefore is exposed to a far higher UV dose. UV penetration of organic polymers has been reported at much greater depths than ion bombardment, for instance >150 μm in polypropylene and ∼15 μm in polybutylene terephthalate.[55] These polymers do not contain native oxygen and as a result show an increase in oxygen after UV treatment when aged in air. UV treatment of PEEK, with wavelengths in the

DOI: 10.1021/acsami.5b06395
ACS Appl. Mater. Interfaces 2015, 7, 23029−23040

range of 250−400 nm, has been found to interact strongly with the aromatic ether bond, resulting in scission of the PEEK monomer.[56] This results in the formation of OH and O−C═O molecules which may either be released from the surface as volatile groups, or recombine to form esters. The modification depth with this radiation was found to be approximately 200 μm−3 orders of magnitude greater than the nitrogen ion penetration. The formation of these compounds at depths of up to 200 μm explains why the oxygen signal did not return to untreated levels with long etch times in XPS analysis. This process would be expected to be treatment time dependent, as UV exposure depends on the time spent in the plasma. Therefore, if UV irradiation is responsible for oxygen release, then the chemical modifications must saturate at exposure times of less than 240 s under the plasma conditions used in this study.

After PIII treatment, the relative concentration of C═O groups in the PIII treated layer decreases, while the relative concentration of C−O groups increases (Figure 10B). Relative concentrations of 50% C═O and 50% C−O can be explained by the presence UV generated O−C═O molecules and esterification of the remaining oxygen. Longer PIII treatments result in an increase in C−O groups and the formation of other low concentration oxygen groups and can be attributed to radical mediated oxidation of the surface.

CONCLUSIONS

Plasma immersion ion implantation was used in this study to modify the surface mechanical properties of PEEK by causing an increase in the Young's modulus and elastic energy recovery, as well as introducing a time dependent aspect to the elastic energy recovery, which saturated with high fluence treatments. Protein immobilization was found to saturate at treatment levels below those investigated here, indicating that the surface mechanical characteristics can be modified for specific applications without compromising the bioactivity. The mechanical properties varied continuously with respect to depth within the treated layer, indicative of a graded layer that is well integrated with the bulk and is unlikely to delaminate during cyclical mechanical testing, a critical feature for orthopedic implant surface treatments. Modification of the substrate by UV irradiation from the nitrogen plasma occurs to a greater depth than the modifications caused by the ion bombardment, and plays a crucial role in oxygen release from deep within the substrate. This treatment represents a promising method for enhancing the surface mechanical properties of PEEK for bioactivation without adversely affecting its attractive bone-like mechanical properties. This suggests that PIII treated PEEK is well suited to be the next-generation advanced material of choice for orthopedic applications.

AUTHOR INFORMATION

Corresponding Author

* E-mail: edgarw@physics.usyd.edu.au.

Author Contributions

The manuscript was written through contributions of all authors. All authors have given approval to the final version of the manuscript.

Funding

The authors would like to acknowledge the Australian Research Council for research funding. Edgar Wakelin was supported during this research by an Australian Postgraduate Award.

Notes

The authors declare no competing financial interest.

ACKNOWLEDGMENTS

The authors would like to thank Dr. Matthew Field from the School of Applied Science, RMIT University, Australia, for his expertise and help in performing XPS experiments.

REFERENCES

(1) Bilek, M. M. M.; Bax, D. V.; Kondyurin, A.; Yin, Y.; Nosworthy, N. J.; Fisher, K.; Waterhouse, A.; Weiss, A. S.; dos Remedios, C. G.; McKenzie, D. R. Free Radical Functionalization of Surfaces to Prevent Adverse Responses to Biomedical Devices. *Proc. Natl. Acad. Sci. U. S. A.* **2011**, *108* (35), 14405−14410.

(2) Wang, H.; Xu, M.; Wu, Z.; Zhang, W.; Ji, J.; Chu, P. K. Biodegradable Poly (butylene succinate) Modified by Gas Plasmas and their In Vitro Functions as Bone Implants. *ACS Appl. Mater. Interfaces* **2012**, *4* (8), 4380−4386.

(3) Shi, W.; Li, X.; Dong, H. Improved Wear Resistance of Ultra-high Molecular Weight Polyethylene by Plasma Immersion Ion Implantation. *Wear* **2001**, *250* (1), 544−552.

(4) Kondyurin, A.; Gan, B. K.; Bilek, M. M. M.; Mizuno, K.; McKenzie, D. R. Etching and Structural Changes of Polystyrene Films During Plasma Immersion Ion Implantation from Argon Plasma. *Nucl. Instrum. Methods Phys. Res., Sect. B* **2006**, *251* (2), 413−418.

(5) Bilek, M. M. M.; Kondyurin, A.; Dekker, S.; Steel, B. C.; Wilhelm, R. A.; Heller, R.; McKenzie, D. R.; Weiss, A. S.; James, M.; Möller, W. Depth-Resolved Structural and Compositional Characterization of Ion-Implanted Polystyrene that Enables Direct Covalent Immobilization of Biomolecules. *J. Phys. Chem. C* **2015**, *119*, 16793.

(6) Dong, H.; Bell, T.; Blawert, C.; Mordike, B. Plasma Immersion Ion Implantation of UHMWPE. *J. Mater. Sci. Lett.* **2000**, *19* (13), 1147−1149.

(7) Valenza, A.; Visco, A.; Torrisi, L.; Campo, N. Characterization of Ultra-high-molecular-weight polyethylene (UHMWPE) Modified by Ion Implantation. *Polymer* **2004**, *45* (5), 1707−1715.

(8) Kondyurin, A.; Nosworthy, N. J.; Bilek, M. M. Attachment of Horseradish Peroxidase to Polytetrafluorethylene (Teflon) after Plasma Immersion Ion Implantation. *Acta Biomater.* **2008**, *4* (5), 1218−1225.

(9) Marletta, G.; Licciardello, A.; Calcagno, L.; Foti, G. Reflection Electron Energy Loss Spectroscopy of keV Bombarded Polystyrene at High Ion Fluences. *Nucl. Instrum. Methods Phys. Res., Sect. B* **1989**, *37*, 712−715.

(10) Kondyurin, A.; Bilek, M. *Ion Beam Treatment of Polymers: Application Aspects from Medicine to Space*. 2nd ed.; Elsevier: Amsterdam, 2014.

(11) Marcondes, A.; Ueda, M.; Kostov, K.; Beloto, A.; Leite, N.; Gomes, G.; Lepienski, C. Improvements of Ultra-high Molecular Weight Polyethylene Mechanical Properties by Nitrogen Plasma Immersion Ion Implantation. *Braz. J. Phys.* **2004**, *34* (4B), 1667−1672.

(12) Svorcik, V.; Rybka, V.; Hnatowicz, V.; Smetana, K., Jr. Structure and Biocompatibility of Ion Beam Modified Polyethylene. *J. Mater. Sci.: Mater. Med.* **1997**, *8* (7), 435−440.

(13) Powles, R.; McKenzie, D.; Meure, S.; Swain, M.; James, N. Nanoindentation Response of PEEK Modified by Mesh-assisted Plasma Immersion Ion Implantation. *Surf. Coat. Technol.* **2007**, *201* (18), 7961−7969.

(14) Díez-Pascual, A. M.; Díez-Vicente, A. L. Nano-TiO2 Reinforced PEEK/PEI Blends as Biomaterials for Load-Bearing Implant Applications. *ACS Appl. Mater. Interfaces* **2015**, *7* (9), 5561−5573.

(15) Hirakawa, K.; Jacobs, J. J.; Urban, R.; Saito, T. Mechanisms of Failure of Total Hip Replacements: Lessons Learned from Retrieval Studies. *Clin. Orthop. Relat. Res.* **2004**, *420*, 10−17.

(16) Wu, S.; Liu, X.; Yeung, A.; Yeung, K. W.; Kao, R.; Wu, G.; Hu, T.; Xu, Z.; Chu, P. K. Plasma-modified Biomaterials for Self-antimicrobial Applications. *ACS Appl. Mater. Interfaces* **2011**, *3* (8), 2851−2860.

DOI: 10.1021/acsami.5b06395
ACS Appl. Mater. Interfaces 2015, 7, 23029−23040

(17) Noyama, Y.; Miura, T.; Ishimoto, T.; Itaya, T.; Niinomi, M.; Nakano, T. Bone Loss and Reduced Bone Quality of the Human Femur after Total Hip Arthroplasty under Stress-Shielding Effects by Titanium-based Implant. *Mater. Trans.* **2012**, *53* (3), 565−570.
(18) Walsh, W.; Bertollo, N.; Christou, C.; Schaffner, D.; Mobbs, R. Plasma Sprayed Titanium Coating to Polyetheretherketone Improves the Bone-Implant Interface. *Spine J.* **2015**, *15*, 1041.
(19) Ma, R.; Tang, S.; Tan, H.; Qian, J.; Lin, W.; Wang, Y.; Liu, C.; Wei, J.; Tang, T. Preparation, Characterization, In Vitro Bioactivity, and Cellular Responses to a Polyetheretherketone Bioactive Composite Containing Nanocalcium Silicate for Bone Repair. *ACS Appl. Mater. Interfaces* **2014**, *6* (15), 12214−12225.
(20) Chrzanowski, W.; Lee, J. H.; Kondyurin, A.; Lord, M. S.; Jang, J. H.; Kim, H. W.; Bilek, M. M. Nano-Bio-Chemical Braille for Cells: The Regulation of Stem Cell Responses using Bi-Functional Surfaces. *Adv. Funct. Mater.* **2015**, *25* (2), 193−205.
(21) San, J.; Zhu, B.; Liu, J.; Liu, Z.; Dong, C.; Zhang, Q. Mechanical Properties of Ion-implanted Polycarbonate. *Surf. Coat. Technol.* **2001**, *138* (2), 242−249.
(22) Dong, H.; Bell, T. State-of-the-art Overview: Ion Beam Surface Modification of Polymers Towards Improving Tribological Properties. *Surf. Coat. Technol.* **1999**, *111* (1), 29−40.
(23) Powles, R.; McKenzie, D.; Fujisawa, N.; McCulloch, D. Production of Amorphous Carbon by Plasma Immersion Ion Implantation of Polymers. *Diamond Relat. Mater.* **2005**, *14* (10), 1577−1582.
(24) Wen, F.; Huang, N.; Sun, H.; Wang, J.; Leng, Y. Synthesis of Nitrogen Incorporated Carbon Films by Plasma Immersion Ion Implantation and Deposition. *Surf. Coat. Technol.* **2004**, *186* (1), 118−124.
(25) Wakelin, E. A.; Kondyurin, A. V.; Wise, S. G.; McKenzie, D. R.; Davies, M. J.; Bilek, M. M. M. Bio-Activation of Polyether Ether Ketone Using Plasma Immersion Ion Implantation: A Kinetic Model. *Plasma Processes Polym.* **2015**, *12*, 180.
(26) Kosobrodova, E.; Kondyurin, A.; McKenzie, D. R.; Bilek, M. M. M. Kinetics of Post-treatment Structural Transformations of Nitrogen Plasma Ion Immersion Implanted polystyrene. *Nucl. Instrum. Methods Phys. Res., Sect. B* **2013**, *304*, 57−66.
(27) Thorwarth, G.; Hammerl, C.; Kuhn, M.; Assmann, W.; Schey, B.; Stritzker, B. Investigation of DLC Synthesized by Plasma Immersion Ion Implantation and Deposition. *Surf. Coat. Technol.* **2005**, *193* (1), 206−212.
(28) Kosobrodova, E. A.; Kondyurin, A. V.; Fisher, K.; Moeller, W.; McKenzie, D. R.; Bilek, M. M. Free Radical Kinetics in a Plasma Immersion Ion Implanted Polystyrene: Theory and Experiment. *Nucl. Instrum. Methods Phys. Res., Sect. B* **2012**, *280*, 26−35.
(29) Oates, T. W.; Pigott, J.; McKenzie, D. R.; Bilek, M. M. Electric Probe Measurements of High-voltage Sheath Collapse in Cathodic Arc Plasmas due to Surface Charging of Insulators. *IEEE Trans. Plasma Sci.* **2003**, *31* (3), 438−443.
(30) Matossian, J. N.; Schumacher, R. W.; Pepper, D. M. *Surface potential control in plasma processing of materials* **1994**.
(31) Shlyakhtenko, L. S.; Gall, A. A.; Weimer, J. J.; Hawn, D. D.; Lyubchenko, Y. L. Atomic Force Microscopy Imaging of DNA Covalently Immobilized on a Functionalized Mica Substrate. *Biophys. J.* **1999**, *77* (1), 568−576.
(32) Vandenberg, E.; Elwing, H.; Askendal, A.; Lundström, I. Protein Immobilization of 3-aminopropyl Triethoxy Silaneglutaraldehyde Surfaces: Characterization by Detergent Washing. *J. Colloid Interface Sci.* **1991**, *143* (2), 327−335.
(33) Yin, Y.; Bilek, M. M.; McKenzie, D. R.; Nosworthy, N. J.; Kondyurin, A.; Youssef, H.; Byrom, M. J.; Yang, W. Acetylene Plasma Polymerized Surfaces for Covalent Immobilization of Dense Bioactive Protein Monolayers. *Surf. Coat. Technol.* **2009**, *203* (10), 1310−1316.
(34) Bilek, M. M. M.; McKenzie, D. R. Plasma Modified Surfaces for Covalent Immobilization of Functional Biomolecules in the Sbsence of Chemical Linkers: Towards Better Biosensors and a New Generation of Medical Implants. *Biophys. Rev.* **2010**, *2* (2), 55−65.
(35) Laemmli, U. K. Cleavage of Structural Proteins During the Assembly of the Head of Bacteriophage T4. *Nature* **1970**, *227* (5259), 680−685.
(36) Hodneland, C. D.; Lee, Y.-S.; Min, D.-H.; Mrksich, M. Selective Immobilization of Proteins to Self-Assembled Monolayers Presenting Active Site-directed Capture Ligands. *Proc. Natl. Acad. Sci. U. S. A.* **2002**, *99* (8), 5048−5052.
(37) Fujisawa, N.; Swain, M. V. Effect of Unloading Strain Rate on the Elastic Modulus of a Viscoelastic Solid Determined by Nano-indentation. *J. Mater. Res.* **2006**, *21* (03), 708−714.
(38) Ha, S.-W.; Hauert, R.; Ernst, K.-H.; Wintermantel, E. Surface Analysis of Chemically-etched and Plasma-treated Polyetheretherketone (PEEK) for Biomedical Applications. *Surf. Coat. Technol.* **1997**, *96* (2), 293−299.
(39) Jama, C.; Dessaux, O.; Goudmand, P.; Gengembre, L.; Grimblot, J. Treatment of Poly (ether ether ketone) (PEEK) Surfaces by Remote Plasma Discharge. XPS Investigation of the Ageing of Plasma-treated PEEK. *Surf. Interface Anal.* **1992**, *18* (11), 751−756.
(40) Graf, N.; Yegen, E.; Gross, T.; Lippitz, A.; Weigel, W.; Krakert, S.; Terfort, A.; Unger, W. E. XPS and NEXAFS Studies of Aliphatic and Aromatic Amine Species on Functionalized Surfaces. *Surf. Sci.* **2009**, *603* (18), 2849−2860.
(41) NIST XPS database. http://srdata.nist.gov/xps/EnergyTypeValSrch.aspx (accessed May 4, 2015).
(42) Waterhouse, A.; Bax, D. V.; Wise, S. G.; Yin, Y.; Dunn, L. L.; Yeo, G. C.; Ng, M. K.; Bilek, M. M.; Weiss, A. S. Stability of a Therapeutic Layer of Immobilized Recombinant Human Tropoelastin on a Plasma-Activated Coated Surface. *Pharm. Res.* **2011**, *28* (6), 1415−1421.
(43) Bax, D. V.; McKenzie, D. R.; Weiss, A. S.; Bilek, M. M. Linker-free Covalent Attachment of the Extracellular Matrix Protein Tropoelastin to a Polymer Surface for Directed Cell Spreading. *Acta Biomater.* **2009**, *5* (9), 3371−3381.
(44) Molazemhosseini, A.; Tourani, H.; Naimi-Jamal, M.; Khavandi, A. Nanoindentation and Nanoscratching Responses of PEEK Based Hybrid Composites Reinforced with Short Carbon Fibers and Nano-silica. *Polym. Test.* **2013**, *32* (3), 525−534.
(45) Kosobrodova, E.; Kondyurin, A.; Chrzanowski, W.; McCulloch, D.; McKenzie, D.; Bilek, M. Optical Properties and Oxidation of Carbonized and Cross-linked Structures Formed in Polycarbonate by Plasma Immersion Ion Implantation. *Nucl. Instrum. Methods Phys. Res., Sect. B* **2014**, *329*, 52−63.
(46) Hirsh, S. L.; McKenzie, D. R.; Nosworthy, N. J.; Denman, J. A.; Sezerman, O. U.; Bilek, M. M. The Vroman Effect: Competitive Protein Exchange with Dynamic Multilayer Protein Aggregates. *Colloids Surf., B* **2013**, *103*, 395−404.
(47) Lanyon, L. Functional Strain in Bone Tissue as an Objective, and Controlling Stimulus for Adaptive Bone Remodelling. *J. Biomech.* **1987**, *20* (11), 1083−1093.
(48) McKenzie, D.; Newton-McGee, K.; Ruch, P.; Bilek, M.; Gan, B. Modification of Polymers by Plasma-based Ion Implantation for Biomedical Applications. *Surf. Coat. Technol.* **2004**, *186* (1), 239−244.
(49) Sofield, C.; Sugden, S.; Ing, J.; Bridwell, L.; Wang, Y. Ion Beam Modification of Polymers. *Vacuum* **1993**, *44* (3), 285−290.
(50) Huang, N.; Yang, P.; Leng, Y.; Wang, J.; Sun, H.; Chen, J.; Wan, G. Surface Modification of Biomaterials by Plasma Immersion Ion Implantation. *Surf. Coat. Technol.* **2004**, *186* (1), 218−226.
(51) Tanaka, D.; Ohshio, S.; Saitoh, H. Nano-indentation for Structural Analysis of Hydrogen and Nitrogen-containing Carbon Films. *Jpn. J. Appl. Phys.* **2000**, *39* (10R), 6008.
(52) Kotál, V.; Švorčík, V.; Slepička, P.; Sajdl, P.; Bláhová, O.; Šutta, P.; Hnatowicz, V. Gold Coating of Poly (ethylene terephthalate) Modified by Argon Plasma. *Plasma Processes Polym.* **2007**, *4* (1), 69−76.
(53) Wagner, A.; Fairbrother, D.; Reniers, F. A Comparison of PE Surfaces Modified by Plasma Generated Neutral Nitrogen Species and Nitrogen Ions. *Plasmas Polym.* **2003**, *8* (2), 119−134.
(54) Hnatowicz, V.; Vacík, J.; Červena, J.; Peřina, V.; Švorcík, V.; Rybka, V. On Anomalous Concentration Depth Profiles of Atoms

DOI: 10.1021/acsami.5b06395
ACS Appl. Mater. Interfaces 2015, 7, 23029−23040

Implanted into Polymers. *Nucl. Instrum. Methods Phys. Res., Sect. B* **1998**, *136*, 568−573.
(55) Gijsman, P.; Meijers, G.; Vitarelli, G. Comparison of the UV-degradation Chemistry of Polypropylene, Polyethylene, Polyamide 6 and Polybutylene Terephthalate. *Polym. Degrad. Stab.* **1999**, *65* (3), 433−441.
(56) Nakamura, H.; Nakamura, T.; Noguchi, T.; Imagawa, K. Photodegradation of PEEK Sheets Under Tensile Stress. *Polym. Degrad. Stab.* **2006**, *91* (4), 740−746.

DOI: 10.1021/acsami.5b06395
ACS Appl. Mater. Interfaces 2015, 7, 23029−23040